Scaling-up of the catalytic stacked wire mesh filters for the abatement of diesel soot

María Laura Godoy, Viviana G. Milt, Eduardo E. Miró, Ezequiel D. Banús

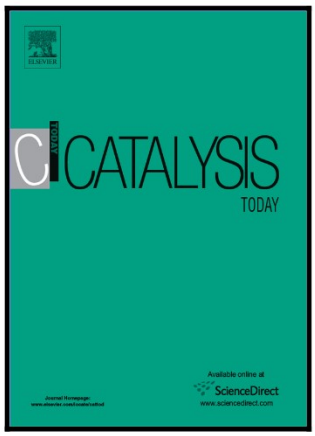

PII: S0920-5861(21)00315-1

DOI: https://doi.org/10.1016/j.cattod.2021.07.010

Reference: CATTOD13433

To appear in: *Catalysis Today*

Received date: 12 March 2021
Revised date: 24 May 2021
Accepted date: 7 July 2021

Please cite this article as: María Laura Godoy, Viviana G. Milt, Eduardo E. Miró and Ezequiel D. Banús, Scaling-up of the catalytic stacked wire mesh filters for the abatement of diesel soot, *Catalysis Today,* (2021) doi:https://doi.org/10.1016/j.cattod.2021.07.010

Scaling-up of the catalytic stacked wire mesh filters for the abatement of diesel soot

María Laura Godoy, Viviana G. Milt, Eduardo E. Miró, Ezequiel D. Banús*

Instituto de Investigaciones en Catálisis y Petroquímica (INCAPE, UNL – CONICET) / Facultad de Ingeniería Química / Universidad Nacional del Litoral, Santa Fe, Argentina

*E-mail: edbanus@fiq.unl.edu.ar

M.L. Godoy: mgodoy@fiq.unl.edu.ar

V.G. Milt: vmilt@fiq.unl.edu.ar

E.E. Miró: emiro@fiq.unl.edu.ar

E.D. Banús: edbanus@fiq.unl.edu.ar

Abstract

This work is based on the development of a stacked AISI 304 stainless steel wire meshes structure with oxidizing and filtering capacity, where the Co and Ce oxide catalysts were deposited on the surface of the metallic fibres as a novel alternative to the current DOC – DPF system. The system was scaled up encouraged by the results obtained at lab scale, going from 16 mm filter diameter to 130 mm. The coated meshes were stacked inside a metallic case in order to conform a catalysed diesel particulate filter (CDPF). A Fiat Palio diesel engine mounted on a test bench was used to evaluate the filtering capacity of the scaled-up wire mesh cartridge. The systems developed were able to reduce particulate matter emitted by diesel engines below limits restrained by laws. The good activity, pressure drop, robustness, versatility and low cost of the designed structures, along with the good adhesion of the catalytic coating, makes them very promising for the development of catalytic filters.

Graphical abstract

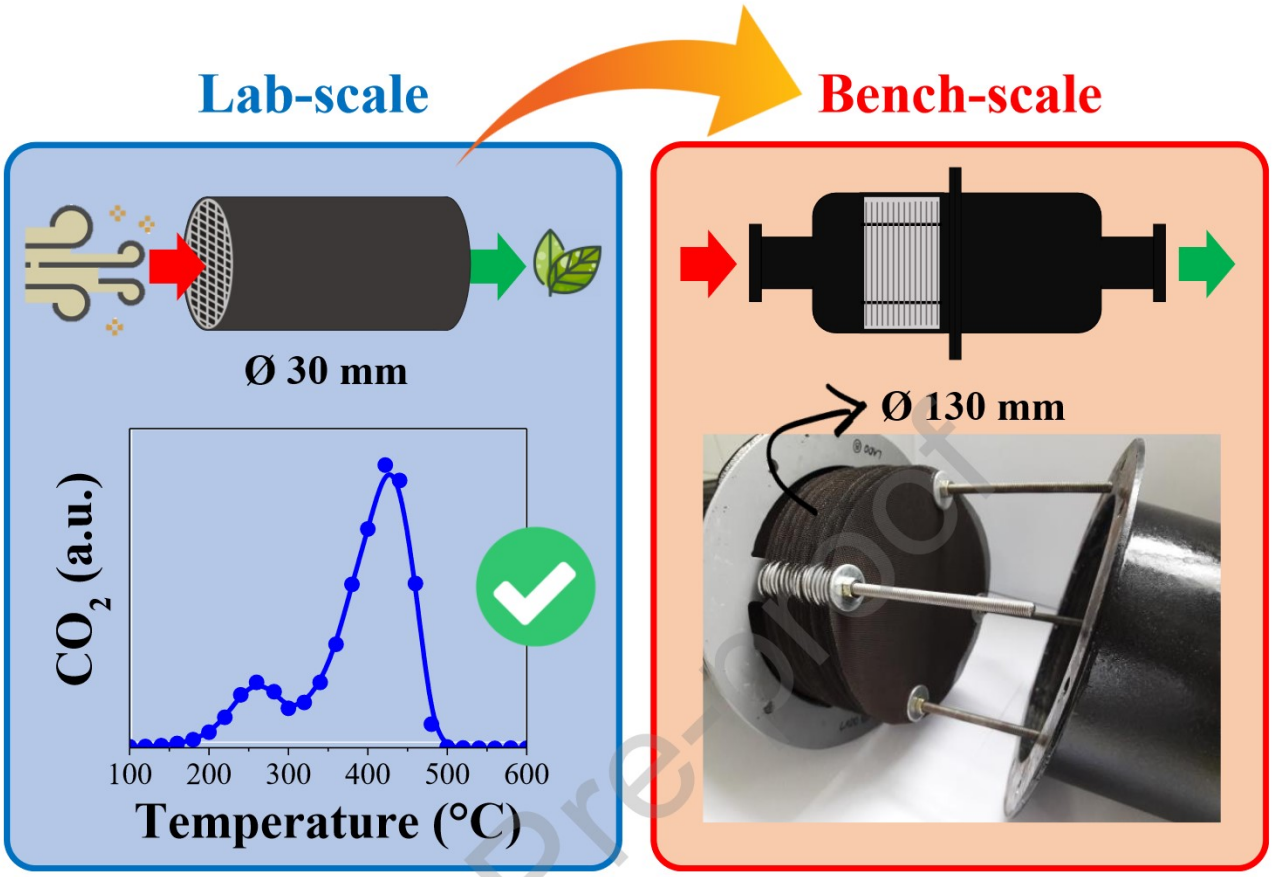

Keywords: wire mesh filter; bench scale; diesel soot combustion; test bench; Catalysed Diesel Particulate Filter

1. Introduction

Diesel engines are commonly used as mechanical engines, power generators and in mobile drives. They find wide spread use in locomotives, construction equipment, automobiles and countless industrial applications, such as marine, mining, telecommunications, underground, agricultural applications, etc. [1]. Their highly thermal efficiency results in less maintenance and low CO_2 emission compared with petrol engines. However, they are being called into question because of their pollutant emissions from the incomplete combustion. Nitrogen oxides (NO_x), unburned hydrocarbon (HC) and carbon monoxide (CO) emitted not only produce well-known impacts on the environment, but also have a negative impact on the human body. Another by-product is particulate matter (PM), which needs to be measured, since carbon-based soot particles are relatively small in size with a large surface and with high potential for adherence that may have adverse health effects. These include the risk of developing asthma and cancer [2]. Moreover, there is growing evidence that exposure to black carbon particles could increase the susceptibility and severity of the coronavirus symptoms by weakening the respiratory system [3–5]. Therefore, more stringent emissions regulations on both PM and particulate number (PN) have been proposed. In order to meet these emissions standards, many strategies like after-treatment systems have

been developed to reduce the engine-out NO_x and PM emissions while maintaining relatively high thermal efficiency [6].

Nowadays, complex and thus expensive systems are used to control the various types of pollutants present in diesel engine exhausts, which include a diesel oxidation catalyst (DOC), a diesel particulate filter (DPF), a selective catalytic reduction unit (SCR) that works with urea injection and an ammonia slip catalyst (ASC) [7]. The combination of a DPF with soot oxidation catalysts, that is, catalytic diesel particulate filter (CDPF), is known as one of the most efficient techniques for soot removal, and highly active oxidation catalysts play a key role in CDPF [8]. This catalytic filter is an alternative that allows particles to be trapped and burned, not requiring fuel post-injections (active filter regeneration). This is based on the fact that catalytic oxidation allows the removal of PM at lower temperatures, which impacts on lower fuel consumption, as the soot particles can be burned in situ in the first units of the purification train (DOC and DPF).

For particulate filters, it is essential to use a structured support resistant to the severe operating engine conditions: high gas flows, thermal shocks and vibrations, and the selected substrate must have filtering characteristics with low pressure drop and high specific surface area to be able to deposit the catalyst [9]. Monoliths have been shown to be useful for gas exhaust treatment [10–12], selective catalytic NO_x reduction [13] and catalytic combustion [14–16]. Wall-flow DPFs are the most common, where the PM removal is achieved by forcing exhaust through porous walls separating adjacent channels in a monolithic substrate. However, the accumulation of soot in the filter walls induces a significant back pressure on the diesel engine, which can cause diesel vehicles to consume more fuel and under worse case scenarios render the engine/vehicle un-operable [17]. Also, the PM growing layer produces narrow channels where laminar flow takes place, thus a mass transfer limitation from the gas phase to the catalytic layer deposited on the channel wall [18].

Alternatively, deep bed filters can be used, constructed with relatively open structure materials compared to surface filters. In these particulate traps, soot is retained in the structure by three well-known mechanisms: inertial interception, Brownian diffusion and flow line interception [19]. The main advantage in using deep bed filters is the enhanced contact soot-catalyst, promoting its continuous regeneration. Deep bed systems can be made from sponges [20] and ceramic papers [12,21], to which the PM is trapped by their tortuosity, as would stacked wire mesh structures [18]. The latter are worth highlighting because of their combination of excellent mass and heat transfer characteristics with low construction costs [22]. Radial mixing of gases occurs through the porous structure of metal meshes, which leads to a more uniform distribution of fluids across the bed diameter [23]. Another advantage of these metallic fibres is their easy scalability. The geometrical flexibility of wire mesh catalysts makes them suitable for adapting to any required shape making them applicable to several industrial and environmental processes. In particular, AISI 304 stainless steel wire mesh is widely used, both for its advantageous mechanical and physical properties, and also for its low cost.

Moreover, CeO_2-based catalysts are probably the most efficient catalysts for diesel soot combustion, used alone or in combination with other materials such as noble metals [24]. The CeO_2 support combines exceptional redox and acid-base properties with oxygen storage capacity, which can be controlled by

appropriate preparation and treatment [25,26]. The presence of cobalt can enhance the reduction of ceria surface oxygen species, resulting in an improvement in the catalytic activity of Co-Ce for NO oxidation and its ability to store NO_2 as surface nitrates [27]. The high NO oxidation activity and high NO_2 storage capacity make the Co-Ce catalyst efficient for NO_x-assisted soot oxidation [28–30]. The suitability of CeO_2-based wire mesh monoliths for the soot treatment has been demonstrated at lab-scale [18,31,32]. In this vein, in a previous work promising results using Co,Ce catalysts deposited on wire mesh monoliths for the simultaneous oxidation of diesel soot and VOCs were reported [33].

The objective of this work is to go further in the study of wire mesh monoliths for the abatement of soot coming from the exhausts of a Fiat Palio engine. To this aim, both laboratory and bench scale filters were developed and a test bench was used to evaluate their performance. The Co,Ce catalytic system was selected for the scaled monolith due to the good activity for the combustion of soot in the laboratory samples. Additionally, the PM retention capacity of different configurations of the bench-scale structure was investigated: with 40 stacked meshes and with the addition of a ceramic paper disc between the last two meshes inside the metal casing. Also, the pressure drop of the scaled monolith was studied, with and without the ceramic paper. The activity of the lab-scale substrates was evaluated by means of TPO experiments, both for the burning of collected bench soot and also for the combustion of soot incorporated through a PM suspension, which was previously obtained by burning commercial diesel fuel. Chemical and morphological characterisation of the structured catalysts was carried out by means of SEM/EDS, LRS, XRD. The soot collected on the ceramic paper after the bench tests was characterised by TGA/DSC.

2. Experimental

2.1. Design and construction of the stacked wire mesh structures

2.1.1. Laboratory scale monolith

Lab-scale structures were prepared according to Montes and co-workers [18,34], 16 mm diameter and 30 mm height, with 30 stacked meshes. AISI 304 stainless steel wire meshes were used, with 500 µm mesh opening and 250 µm wire diameter (wire mesh size: 34), 44% front void fraction and 21 cm^2/g geometric surface area [33]. The wire meshes were stacked inside a stainless steel cartridge [31]. The stacked wire mesh monoliths were first washed in water – detergent in an ultrasonic bath during 30 min, and then in acetone under the same conditions, drying them at 130 °C for 2 h in an oven after each washing step. After that, the samples were calcined at 900 °C – 1 h, as described in a previous work [31].

2.1.2. Bench scale monolith

Wire mesh preparation: The same wire mesh type mentioned above was used to prepare 130 mm diameter discs. For this reason, a stainless-steel punching device was built. The piece was tempered and coated with antioxidant paint. After that, the wire mesh discs were cut employing a hydraulic press (**Figure 1S**). Once the meshes were cut, four holes 7 mm diameter were made in each one with a punch (**Figure 1**), and then stacked inside the cartridge, as it will be shown below.

Next, the meshes were first washed with detergent – water and then in acetone in ultrasonic bath. They were dried at 130 °C, then stacked in the muffle and calcined at 900 °C – 1 h. The samples were weighed after cooling down to room temperature.

Metal housing construction: A metal casing was designed in a way it can allow the stacking of 40 wire mesh discs. **Figure 2** shows a cylindrical metal chamber 140 mm diameter and 310 mm length, constructed from the recycling of two air dryer cases (**Figures 2S** and **3S**). Wire meshes were arranged inside the casing by piling them through four steel bars (20 meshes placed on each side). As the meshes must have a slight separation between them to generate a tortuous path and thus avoiding preferential paths, four washers were placed when stacked inside the metal casing. The complete bench scale monolith can be seen in **Fig. 2**. Additionally, a ceramic paper disc was placed at the bottom of the casing in order to help collecting soot particles (**Fig. 2c**). This sheet was prepared by the papermaking technique and consisted in a disc of silica-alumina fibres (130 mm diameter and 5 mm height – see **Fig. 4S** in Supplementary Data). A thorough description of the paper preparation and its properties are described elsewhere [35].

2.2. Catalyst preparation and washcoating of the structures

The catalytic system selected was Co,Ce, therefore 400 ml of an equimolar suspension was prepared according to a previous work [33]. The Co,Ce suspension was composed of CeO_2 nanoparticles (Sigma–Aldrich®), CeO_2 commercial colloidal suspension (Nyacol®, 20 w/wt %, $d_{particle}$ = 10–20 nm, pH = 3), PVA (Poly vinyl alcohol, Sigma–Aldrich®, P1763 – Av. mol. wt. = 70.000 g/mol) and Co_3O_4 nanoparticles (Sigma–Aldrich®, $d_{particle}$ < 50 nm). Briefly, 8 mg of PVA were dissolved in 400 ml of deionized water, previously heated at 70 °C under magnetic stirring. Afterwards, 50 g of CeO_2 colloidal suspension, 10 g of CeO_2 and 9.32 g of Co_3O_4 nanoparticles were slowly added to the aqueous solution at room temperature. The suspension remained under stirring during 24 h. The mass ratio between the components (H_2O:PVA:CeO_2 nanop.:colloidal CeO_2:Co_3O_4 nanop.) was 40:0.8:1:5:0.9, so as to achieve a Ce:Co molar ratio = 1:1.

2.2.1. Lab scale monolith

Before the coating procedure, the external surface of the structures was masked with Teflon® tape and heat-shrinkable tape to favour the catalyst anchoring preferentially on the wire meshes and the internal area of the cylinder. The washcoating technique was applied by immersing the metallic substrates in the Co,Ce suspension during 1 min. The excess of slurry was removed by centrifugation (600 rpm – 3 min). After this, the structures were dried at 130 °C – 1 h and then weighted. The immersion, centrifugation, drying and weighing process was repeated until 220 mg of total catalyst (Co + Ce) was loaded. Finally, the coated substrates were calcined at 600 °C for 2 h (heating rate: 1 °C/min) [33]. The coated monoliths obtained were named as *Co,Ce-m.*

In addition to the structured system, the Co,Ce powder formulation was prepared from drying the suspension used for the immersion of the monolith and calcining the powder at 600 °C for 2 h (heating rate: 1 °C/min). The catalyst thus obtained was named *Co,Ce-P.*

2.2.2. Bench scale monolith

The wire mesh discs were immersed horizontally in the Co,Ce suspension for 1 min and most of the supernatant was removed by air blowing with a hair dryer. An air gun connected to a synthetic air tube was used to remove the remaining suspension retained in the spaces between the wires. The meshes were placed in the oven at 130 °C – 1 h and then weighed. The immersion cycle was repeated until ≈ 250 mg of total catalyst per mesh was loaded. It should be mentioned that the amount of catalyst incorporated in the wire mesh discs per geometric area is similar in both lab (16 mm diameter) and bench (130 mm diameter) scales. Finally, the coated discs were calcined at 600 °C. The bench scale monolith with 40 stacked catalytic meshes inside the case was denominated *Co,Ce-MC* (or *MC*, when containing 40 bare stacked meshes).

2.3. Catalyst characterisation

Scanning electron microscopy (SEM) images and energy dispersive X-ray spectroscopy (EDS) were taken on a Phenom World Pro X equipment (10 kV and 20 kV acceleration voltage, respectively). The wire mesh samples were previously gold-covered by sputtering. It was necessary to break and open the lab scale structures to obtain the metallic samples and evaluate the homogeneity of the coating along the monolith.

The adherence between the catalyst coating and the metallic substrate was evaluated by ultrasonication tests. The coated wire mesh (130 mm diameter) was immersed in acetone and subjected to ultrasonication for different times. Then, the sample was dried for 1 h at 130 °C and weighed after each step. Following, a mechanical stress test of the coated wire mesh was performed, which consisted of repeatedly mesh twisting and weighing to study the detachment of the catalytic layer.

The X-Ray diffraction (XRD) patterns of the powdered and structured catalysts were recorded with a PANalytican Empyrean instrument with Cu Kα radiation (40 kV, 45 mA) over a 2θ range of 20–80°, at a scan rate of 2°/min.

Raman spectra were collected using a Horiba Jobin Ybon LabRAM HR instrument. The excitation wavelength was 532.13 nm and the laser power, 30 mW.

Pressure drop measurements of the bench scale monolith were performed in a Flujo Tech 600 flowmeter (Horacio Resio Devices), which is used for flow analysis in real engines [36], so that it was necessary to build a device to hold the monolithic sample. The software program of the equipment displayed the flow curves for different air pressure values. Pressure drop tests of the lab scale monoliths were published in a previous work [33].

Thermogravimetric analysis was performed to measure the mass variation of the sample during controlling atmosphere. A sample of 10 mg was used in all experiments and conducted in a TGA/SDTA851e Mettler Toledo® instrument. Measurements were carried out in circulating N_2 or industrial grade air with a flow rate of 30 cm^3/min.

DSC experiments were conducted in the TGA/DSC instrument mentioned above, in an air atmosphere with a flow rate of 30 cm^3/min. Samples of 10 mg were used. TGA/DSC analysis were performed at a temperature range from 25 °C to 600 °C, with a heating ramp of 10 °C/min. Then, it was kept at 600 °C for 10 min.

2.4. Filtration capability

The scaled-up monolith filtration capability, which refers to the ability of retaining soot particles throughout the filter, was studied by means of opacity measurements carried out in a test bench with or without the filter. The test bench (**Fig. 3**) consisted of a four stoke, indirect injection turbocharged FIAT diesel engine (number of cylinders = 4, displacement = 1910 cm^3, bore = 82.6 mm, stroke = 90 mm, compression ratio = 19.2:1, maximum power = 82 CV at 4000 rpm, maximum torque = 173 Nm at 2800 rpm). The opacity of the exhaust smoke was measured with an OPABOX Autopower Smokemeter and the protocol followed was provided by the Emission Test Software (ETS), which interacts automatically with the opacity meter and the Revolution Counter 3 (RC3) tools. This test consisted in a series of rapid engine accelerations from idle to governed speed, whereas the relative opacity (% or m^{-1}) was displayed by the software program. So as to study the filtration capacity of the scaled-up system, measures have been made before and after the addition of the wire mesh monolith to the engine exhaust pipe. Besides, the system was tested with 40 stacked wire meshes (*MC*) and with 40 discs plus the addition of a silica-alumina paper disc between the last two stacked meshes (*MC + paper*). The role of the ceramic paper was to help collecting soot particles generated under normal diesel engine operating conditions for further characterization studies (thermogravimetric analysis and TPO experiments, Section 3.4.1).

2.5. Diesel soot combustion experiments

Diesel soot was obtained either at bench or laboratory scale, the first one generated by the diesel engine, and the second one by combustion of diesel fuel inside a glass flask. Euro V diesel fuel containing less than 10 ppm-wt. sulphur was used in this study.

2.5.1. Bench scale (bench soot)

The samples Co,Ce-m and silica-alumina paper (ceramic paper without catalyst) with soot obtained from the bench test under the real operating conditions of a diesel engine were studied in the laboratory by means of TPO experiments.

Ceramic paper: Samples of the ceramic paper with particulate from the test bench were taken and characterised by TGA and DSC experiments in order to study thermal evolutions in oxidising atmosphere (air). Also, 16 mm diameter discs were cut with a punch and evaluated in the TPO equipment.

Wire mesh monolith*:* In order to collect soot particles from the test bench in aerosol form, the construction of an AISI 316 stainless steel device was necessary to hold the laboratory-scale stacked wire mesh monolith. This adaptor was located in an outlet of the exhaust pipe, and has an exit that allows the connection to a vacuum system to force the flow of gases emitted through the cartridge (see **Figure 4**). Hence, soot particles were accumulated in the wire mesh sample after 75 min of engine ignition

2.5.2. Laboratory scale (lab soot)

Soot particles were collected from the vessel walls after the burning of commercial diesel fuel (YPF, Argentina). Then, they were dried at 120 °C for 72 h [37] and dispersed in *n*-hexane using an ultrasonic bath. This 3000-ppm suspension was used to incorporate particulate matter to both Co,Ce-m and silica-alumina paper.

Ceramic paper: Three discs 16 mm diameter were impregnated with the soot suspension by dripping over the surface, then were dried overnight at room temperature.

Wire mesh monolith: The lab-scale cartridges were loaded with soot according to a previous work [31].

2.5.3. TPO experiments

The tubular quartz reactor (16 mm diameter) was fed with 20 ml/min of a mixture of O_2 (18%) and NO (0.1%), He balance, and heated from room temperature to 600 °C (5 °C/min). The CO_2 produced by the combustion was analysed using a Shimadzu GC-2014 gas chromatograph equipped with a Porapak Q column.

3. Results and discussion

3.1. Catalytic coating

The pre-treatment at 900 °C applied to the lab and bench scale metal structures generated a rough layer composed of oxide spinels, allowing the subsequent anchoring of the Co,Ce catalyst to the substrate [38]. In **Fig. 5** is shown the number of coating cycles (immersion – centrifugation – drying – weighing) needed to load the desired catalyst mass per cm^2 of mesh in the lab-scale monoliths (Co,Ce-m) (**Fig. 5a**) and in the wire mesh discs (Co,Ce-M) (**Fig. 5b**). It should be noted that **Fig. 5b** shows the average of 40 meshes impregnated with catalyst. Whereas two impregnation steps were necessary to load 250 mg catalyst per cm^2 wire mesh for the Co,Ce-lab scale monoliths (**Fig. 5a**), four cycles per mesh were required to coat the bench scale wire meshes (**Fig. 5b**). This difference can be attributed to the different methods used to remove the excess of suspension in each sample. The Co,Ce mass loaded per mesh area in both samples increased almost linearly with successive coatings.

The morphology of the catalyst coating was studied by SEM, as it is shown in **Fig. 6**. The upper and intermediate meshes of the Co,Ce-m cartridge were analysed to study the homogeneity of the coating along the monolith. The images obtained show a homogeneous film covering the AISI 304 stainless steel mesh, revealing the formation of micrometric aggregates of Co_3O_4 and CeO_2 particles. Moreover, **Fig. 6** also presents EDS mapping pictures of the different meshes, suggesting a uniform distribution of the elements along the metallic fibres. Atomic ratios of the components detected in the EDS mapping studies were considered in a previous work [33].

The stability of the catalyst coating has been evaluated via ultrasound method, as described previously. Both a Co,Ce-monolith (Co,Ce-m) and a Co,Ce coated mesh (130 mm diameter – Co,Ce-M) were immersed in acetone during 4 h and submitted to ultrasound, showing a retention of the catalytic layer of over 75.9 and 97.6%, respectively (**Fig. 7**). As observed, the scaled-up catalytic mesh (Co,Ce-M) showed

a very good retention of the catalytic coating, whereas the small meshes stacked into the small monolith (Co,Ce-m) showed lower retention. As studied in a previous work, the adherence of the catalytic layer depended on the number of wire-mesh discs. The higher the number of wire-mesh discs, the higher the adherence of the catalytic layer. However, after the structure coatings, some catalyst accumulations were observed in the internal surface of the cartridge and on the external part of the mesh cover welded to the cartridge, which disappeared after the adherence test [18]. According to this, the Co,Ce-m cartridge loses these accumulated fractions of catalyst during the first part of the stability test, showing a stable coating on wire meshes after 150 min. Furthermore, the Co,Ce-M treated mesh was folded several times, as depicted in **Fig. 8**, in order to analyse the possible detachment of the catalytic layer. Nevertheless, the weight remained unchanged.

In order to identify the crystalline phases present, XRD patterns were obtained for Co,Ce powdered, lab and bench scale structured catalysts (**Fig. 9**). In the case of the lab scale monoliths, the cartridges were dismantled to analyse the first two meshes (meshes 2 and 3) and the two intermediate meshes (meshes 15 and 16). However, **Fig. 9b** shows the diffractograms of a single sample per structure, since the results obtained were identical. For bench scale samples, individual 130 mm diameter wire meshes were studied. In the diffractogram corresponding to the catalytic powder Co,Ce-P (**Fig. 9a**), the signals at 2θ = 31.3°, 36.9°, 38.5°, 44.8°, 59.4° and 65.3° were detected, belonging to the crystalline phases Co_3O_4 of the cubic spinel type (JCPDS 42-1467) [39] and CeO_2 of the cubic fluorite type (JCPDS 34-394) at 2θ = 28.6°, 33.1°, 47.6°, 56.4°, 59.2°, 69.5°, 76.8° and 79.2° [40]. **Figs. 9b** and **c** show the corresponding XRD patterns of both the catalytic and bare calcined lab scale monoliths (Co,Ce-m and Calcined m) and individual catalytic and bare scaled-up calcined wire meshes (Co,Ce-M and Calcined M). It can be observed that the pre-treatment at 900 °C produces a surface of similar composition and roughness both on the laboratory-scale monolith (**Fig. 9b** – Calcined m) and the scaled-up metal mesh (**Fig. 9c** – Calcined M). For which the calcination of the complete lab scale monolith produces surface characteristics similar to those obtained when calcining individual scaled-up wire meshes. For both samples, the phases present in the oxide layer were attributed to chromium III oxide (Cr_2O_3, JCPDS 38-1479), manganese-chromium spinel ($Mn_{1+x}Cr_{1-x}O_{4-x}$, JCPDS 33-892), chromium-iron spinel ($FeCr_2O_4$, JCPDS-34-140) and iron III oxide (Fe_2O_3, JCPDS 33-664) [38,41,42]. When the catalyst was incorporated in the structured substrates, in the diffractograms appeared not only the signals of the Co,Ce catalyst (not marked in **Figs. 9b** and **c**), but also those corresponding to the stainless steel AISI 304 [43] for both the lab scale monolith (**Fig. 9b** – Co,Ce-m) and the scaled-up wire mesh (**Fig. 9c** – Co,Ce-M). The crystalline structure of the stainless steel consists of a mixture of austenite (γ) and martensite (α'), as indicated in **Figs. 9b and c**.

The results of the structural characterisation of powdered and structured catalysts obtained by Raman spectroscopy are shown elsewhere [33]. In the case of the Co,Ce-P sample, Raman spectra revealed bands corresponding to CeO_2 and Co_3O_4 [44]. These signals could also be seen in the upper and intermediate meshes of the Co,Ce-m monolith, and in the Co,Ce-M sample, in accordance with the characterisation by XRD.

3.2. Pressure drop

Pressure drop measurements were carried out with the empty housing (blank), and with 40 stacked wire meshes (20 on each side) with and without catalyst (Co,Ce-MC and MC, respectively). In addition, experiments with MC and Co,Ce-MC configurations were made with the addition of an Al_2O_3 ceramic paper disc at the end of the bed, between the last two metallic meshes, as shown in **Fig. 10**. In the results obtained for different air velocities, it can be seen the curves obtained when graphing ΔP/L (Pa/m) as a function of u (m/s), where L is the bed height (120 mm for the configuration with 40 stacked meshes, or 120.5 mm when the ceramic paper is also present – see **Fig. 2c**). The pressure drop values increase slightly after the addition of the Co,Ce catalyst (Co,Ce-MC) due to the flow area decrease. Furthermore, the ceramic paper disc added between the last two stacked wire meshes of the monolith resulted in an increase of ΔP. However, the high u-values obtained in all cases indicate a low resistance to gas flow of the wire mesh structures. Additionally, in Supplementary Data (**Fig. 5S**) the verification of the Payri equation for diesel particulate filters [45] is observed as straight lines were obtained when plotting ΔP/Q vs Q. It should be mentioned that these stacked wire mesh filters generate similar or lower pressure drop than commercial systems (SiC, aluminium or cordierite filters) [46].

3.3. Opacity measurements

The experiences were carried out on the same day, to guarantee identical environmental conditions, so as to ensure repeatability and comparability of the results obtained from the experiments.

The testing was performed at an engine speed of 3000 rpm, without load, with and without the addition of the filter in the exhaust pipe. In the first case it was not possible to obtain opacity values due to the saturation of the opacimeter lens. **Fig. 11** shows the results obtained from the 20 experiments when the filter had 40 stacked meshes (MC) and another 20 when the ceramic paper was added (MC + paper). It can be seen that the average opacity for the M configuration (**Table 1**) decreases when the ceramic paper is present. In Argentina, the opacity limit value for diesel fumes allowed is 2.62 m^{-1} (65% on a linear scale) (in opacimeter with an effective optical path length of 0.41 m) for 1994 model vehicles and later [47]. In **Table 1** it can be seen that the opacity values obtained for both configurations comply with current regulations, being the opacity of the MC system ten times lower than the established limit value.

3.4. Study of the bench soot

The samples Co,Ce-m and silica-alumina paper (without catalyst) with soot obtained from the test bench under the real operating conditions of a diesel engine were studied in the laboratory.

3.4.1. Soot collected on the ceramic paper disc

Samples of the ceramic paper with bench soot (**Fig. 12**) were taken and characterised by thermogravimetric (TGA) and DSC experiments in order to study thermal evolutions in oxidising atmosphere (air). Also 16 mm diameter discs were cut with a punch and evaluated in the TPO equipment.

TGA and DSC characterisation: When analysing the bench soot (**Fig. 13**), a decrease in mass between 200 and 400 °C was found in the thermogram (red curve), accompanied by an exothermic evolution with the maximum at 333.6 °C observed in the corresponding DSC profile (blue curve). Another mass loss in the range of 400 – 600 °C was observed in the TGA curve, associated with an exothermal peak with a

maximum at 566 °C in the DSC profile. According to the TGA profile, the peak at 333.6 °C of the DSC curve would correspond to the oxidation of the hydrocarbons adsorbed on the diesel soot particles, while the peak observed at higher temperature corresponds to the non-catalytic oxidation of the carbonaceous core of the soot particles.

Catalytic activity: **Fig. 14** shows the TPO profiles of the non-catalytic combustion of soot deposited in aerosol form on the ceramic paper (bench soot, colour red), and of the discs impregnated with soot from a 3000-ppm suspension by dripping (lab soot, colour blue). It can be seen that lab soot and bench soot samples show maxima at 551 °C and 570 °C respectively, which would correspond to the non-catalytic soot burning temperature. The test bench sample also shows a wide signal at lower temperature (250 – 400 °C), which would be associated with the burning of the adsorbed hydrocarbons around the carbonaceous nucleus of the soot particle. Similar results of the non-catalytic combustion of soot were reported in the literature: T_{50} = 575 °C for engine soot and 610 °C for both Printex-U carbon black and flame soot (FS100) [48].

3.4.2. Soot collected on the wire mesh monolith

The soot loaded cartridge extracted from the test bench after the 75 min run (see Experimental 2.5.1) was evaluated by a TPO experiment. **Fig. 15** shows the catalytic curves obtained for the monolith Co,Ce-m with bench soot (**Fig. 15a**) and with soot incorporated from a *n*-hexane suspension (lab soot – **Fig. 15b**).

The deconvolution of the peaks in **Fig. 15** shows four contributions, which from lower to higher temperatures would correspond to the burning of adsorbed hydrocarbons (VOCs), the combustion of hydrocarbons which compose soot structure (SOF fraction of soot), the burning of amorphous carbon and the combustion of graphitic carbon. These contributions appear at 260, 253, 400 and 440 °C, respectively for lab soot, whereas they appear at 269, 335, 440 and 500 °C for bench soot. The shift to higher temperatures observed for bench soot could be ascribed to a less intimate contact between the soot particles and the catalyst (looser contact). Additionally, lab soot exhibits a lower amount of SOF fraction due to the higher temperature reached during the soot obtention process.

In order to further insight into the assignments of the deconvoluted peaks, it is convenient to take into account that soot particles from a diesel engine exhaust pipe are mainly composed of carbon, whose constituent spheres adsorb unburned hydrocarbons and other combustion products (nitrogen and sulphur oxides). A soluble organic fraction (SOF) of a wide range of hydrocarbons is also present in soot [49,50]. Setiabudi et al. compared the TPO profiles of soot produced under normal operating conditions of a diesel engine and a model soot (Printex U), and found that the profile corresponding to real soot had a shoulder at about 227 °C (500 K), which is assigned to the adsorbed hydrocarbons that increase the reactivity [51]. Taking this into consideration, the two lower temperature peaks (269 and 335 °C) of the bench soot sample correspond to the combustion of adsorbed hydrocarbons (SOF) around the soot particle, as previously considered. For the lab soot, the peak at 260 °C corresponds to the burning of the *n*-hexane.

The contributions of two types of carbon were detected by Raman laser spectroscopy in both samples [52]: graphite and amorphous, whereas amorphous carbon burns easier than graphite carbon, which

influences the TPO assessments. Lab soot was found to have a higher proportion of graphitic carbon, and bench soot a higher content of amorphous carbon.

In this way, the Co,Ce catalyst deposited on the metallic cartridges showed to be efficient both for the combustion of the carbonaceous and hydrocarbon fractions of soot. This encourages us to carry out further studies at bench scale.

4. Conclusions

Catalytic monoliths were developed by coating AISI 304 stainless steel wire meshes with a CeO_2 and Co_3O_4 catalytic film, housed in a steel casing. The bench scale system is easy to manufacture in the country and cheaper than an imported filter. Also, the good catalytic activity for soot combustion would allow passive regeneration of the filter under real conditions. This is encouraging to continue studying the self-regeneration of the system with the operating and under load engine. Regarding pressure drop, the close or lower values generated by stacked wire mesh filters compared to commercial systems (SiC, aluminium titanate or cordierite filters) and the versatility of the structure make it easily adaptable to different housing geometries, and therefore to different vehicles. This is a crucial point for the design of exhaust systems, as space in the vehicle is limited. The robustness, versatility and low cost of the designed structures, together with the excellent adhesion of the catalytic coating, allow to extend its application spectrum for the removal of PM from stationary sources.

Acknowledgements

The authors wish to acknowledge the financial support received from Agencia Nacional de Promoción Científica y Tecnológica (ANPCyT), Consejo Nacional de Investigaciones Científicas y Técnicas (CONICET), Agencia Santafesina de Ciencia, Tecnología e Innovación (ASaCTeI) and Universidad Nacional del Litoral (UNL).

References

[1] Why use diesel? Advantages and benefits - How diesel engines and generators work, https://www.generatorsource.com/why_use_diesel.aspx (accessed February 1, 2021).

[2] P. Nagy, I. Zsoldos, A Review on the differences between particle emission, filtration and regeneration of particulate filters of diesel and gasoline engines, Lect. Notes Mech. Eng. 22 (2021) 158–173.

[3] T. Brewer, The future of transportation emission issues, SpringerBriefs Appl. Sci. Technol. (2021) 97–103.

[4] S. Comunian, D. Dongo, C. Milani, P. Palestini, Air pollution and COVID-19: The role of particulate matter in the spread and increase of COVID-19's morbidity and mortality, Int. J. Environ. Res. Public Health 17 (2020) 1–22.

[5] X. Wu, R.C. Nethery, M.B. Sabath, D. Braun, F. Dominici, Air pollution and COVID-19 mortality in the United States: Strengths and limitations of an ecological regression analysis, Sci. Adv. 6 (2020) 1–7.

[6] X. Wang, Y. Wang, Y. Bai, Q. Duan, Properties and oxidation of exhaust particulates from dual fuel combustion: A comparative study of premixed gasoline, n-butanol and their blends, Environ. Pollut. 271 (2021) 116391.

[7] S. Trivedi, R. Prasad, A four-way catalytic system for control of emissions from diesel engine, Sādhanā 43 (2018) 130.

[8] M. Wang, Y. Zhang, Y. Yu, W. Shan, H. He, Cesium as a dual function promoter in Co/Ce-Sn catalyst for soot oxidation, Appl. Catal. B Environ. 285 (2021) 119850.

[9] S. Govender, H.B. Friedrich, Monoliths: A review of the basics, preparation methods and their relevance to oxidation, Catalysts 7 (2017) 62.

[10] R.M. Heck, R.J. Farrauto, Automobile exhaust catalysts, Appl. Catal. A Gen. 221 (2001) 443–457.

[11] R.J. Farrauto, R.M. Heck, Catalytic converters: State of the art and perspectives, Catal. Today 51 (1999) 351–360.

[12] E. Meloni, V. Palma, Most recent advances in diesel engine catalytic soot abatement: Structured catalysts and alternative approaches, Catalysts 10 (2020) 1–27.

[13] R.M. Heck, Catalytic abatement of nitrogen oxides-stationary applications, Catal. Today 53 (1999) 519–523.

[14] R.M. Heck, S. Gulati, R.J. Farrauto, The application of monoliths for gas phase catalytic reactions, Chem. Eng. J. 82 (2001) 149–156.

[15] J.W. Geus, J.C. Van Giezen, Monoliths in catalytic oxidation, Catal. Today 47 (1999) 169–180.

[16] D.F.M. Santos, O.S.G.P. Soares, J.L. Figueiredo, O. Sanz, M. Montes, M.F.R. Pereira, Preparation of ceramic and metallic monoliths coated with cryptomelane as catalysts for VOC abatement, Chem. Eng. J. 382 (2020) 122923.

[17] K. Yang, J.T. Fox, R. Hunsicker, Characterizing diesel particulate filter failure during commercial fleet use due to pinholes, melting, cracking, and fouling, Emiss. Control Sci. Technol. 2 (2016) 145–155.

[18] E.D. Banús, O. Sanz, V.G. Milt, E.E. Miró, M. Montes, Development of a stacked wire-mesh structure for diesel soot combustion, Chem. Eng. J. 246 (2014) 353–365.

[19] B.A.A.L. Van Setten, M. Makkee, J.A. Moulijn, Science and technology of catalytic diesel particulate filters, Catal. Rev. - Sci. Eng. 43 (2001) 489–564.

[20] E. Vanhaecke, C. Pham-Huu, D. Edouard, Simulation and experimental measurement of dynamic behavior of solid foam filter for diesel exhaust gas, Catal. Today 189 (2012) 101–110.

[21] N. Sacco, E. Banús, V. Milt, E. Miró, J.P. Bortolozzi, Catalytic paper filters for diesel soot abatement: Studies at laboratory and bench scales, Emiss. Control Sci. Technol. 6 (2020) 450–461.

[22] A. V. Porsin, A. V. Kulikov, V.N. Rogozhnikov, A.N. Serkova, A.N. Salanov, K.I. Shefer, Structured reactors on a metal mesh catalyst for various applications, Catal. Today 273 (2016) 213–220.

[23] K.S. Chung, Z. Jiang, B.S. Gill, J.S. Chung, Oxidative decomposition of o-dichlorobenzene over V_2O_5/TiO_2 catalyst washcoated onto wire-mesh honeycombs, Appl. Catal. A Gen. 237 (2002) 81–89.

[24] A. Bueno-López, Diesel soot combustion ceria catalysts, Appl. Catal. B Environ. 146 (2014) 1–11.

[25] D. Fino, S. Bensaid, M. Piumetti, N. Russo, A review on the catalytic combustion of soot in diesel particulate filters for automotive applications: From powder catalysts to structured reactors, Appl. Catal. A Gen. 509 (2016) 75–96.

[26] B. Sawatmongkhon, K. Theinnoi, T. Wongchang, C. Haoharn, C. Wongkhorsub, E. Sukjit, A. Tsolakis, Catalytic oxidation of diesel particulate matter by using silver and ceria supported on alumina as the oxidation catalyst, Appl. Catal. A Gen. 574 (2019) 33–40.

[27] V.G. Milt, C.A. Querini, E.E. Miró, M.A. Ulla, Abatement of diesel exhaust pollutants: NO_x adsorption on $Co,Ba,K/CeO_2$ catalysts, J. Catal. 220 (2003) 424–432.

[28] M.Á. Stegmayer, S. Irusta, E.E. Miró, V.G. Milt, Electrospinning synthesis and characterization of nanofibers of Co, Ce and mixed Co-Ce oxides. Their application to oxidation reactions of diesel soot and CO, Catal. Today (2021) In press.

[29] J. Xu, G. Lu, Y. Guo, Y. Guo, X. Gong, A highly effective catalyst of $Co-CeO_2$ for the oxidation of diesel soot : The excellent NO oxidation activity and NO_x storage capacity, Appl. Catal. A Gen. 535 (2017) 1–8.

[30] N.A. Sacco, E.D. Banús, J.P. Bortolozzi, V.G. Milt, E.E. Miró, Ultrasound-assisted deposition of $Co-CeO_2$ onto ceramic microfibers to conform catalytic papers: Their application in engine exhaust treatment, ACS Omega 3 (2018) 18334–18342.

[31] M.L. Godoy, E.D. Banús, O. Sanz, M. Montes, E. Miró, V.G. Milt, Stacked wire mesh monoliths for the simultaneous abatement of VOCs and diesel soot, Catalysts 8 (2018) 16.

[32] A. Vembathu Rajesh, C. Mathalai Sundaram, V. Sivaganesan, B. Nagarajan, S. Harikishore, Emission reduction techniques in CI engine with catalytic converter, Mater. Today Proc. 21 (2020) 98–103.

[33] M.L. Godoy, E.D. Banús, E.E. Miró, V.G. Milt, Single and double bed stacked wire mesh cartridges for the catalytic treatment of diesel exhausts, J. Environ. Chem. Eng. 7 (2019) 103290.

[34] O. Sanz, E.D. Banús, A. Goya, H. Larumbe, J.J. Delgado, A. Monzón, M. Montes, Stacked wire-mesh monoliths for VOCs combustion: Effect of the mesh-opening in the catalytic performance, Catal. Today (2017) 0–1.

[35] A. Sánchez, V.G. Milt, E.E. Miró, R. Güttel, Ceramic fiber-based structures as catalyst supports: a study on mass and heat transport behavior applied to CO_2 methanation, Ind. Eng. Chem. Res. 59 (2020) 16539–16552

[36] Flujometro Flujotech 250 y 600 – HoracioResio.com, http://www.horacioresio.com/flujometro-flujotech-250-y-600/ (accessed December 7, 2017).

[37] V.G. Milt, E.D. Banús, M.A. Ulla, E.E. Miró, Soot combustion and NO_x adsorption on Co,Ba,K/ZrO_2, Catal. Today 133–135 (2008) 435–440.

[38] J.P. Bortolozzi, E.D. Banús, V.G. Milt, L.B. Gutierrez, M.A. Ulla, The significance of passivation treatments on AISI 314 foam pieces to be used as substrates for catalytic applications, Appl. Surf. Sci. 257 (2010) 495–502.

[39] J.C. Medina, S.E. Rodil, R. Zanella, Synthesis of a CeO_2/Co_3O_4 catalyst with a remarkable performance for the soot oxidation reaction, Catal. Sci. Technol. 10 (2020) 853–863.

[40] S.M. Lee, G.J. Kim, S.H. Lee, I.H. Hwang, S.C. Hong, S.S. Kim, Catalytic performance of $Ce_{0.6}Y_{0.4}O_2$-supported platinum catalyst for low-temperature water−gas shift reaction, ACS Omega 3 (2018) 3156–3163.

[41] A.A. Ali, M. Madkour, F.A. Sagheer, M.I. Zaki, A.A. Nazeer, Low-Temperature catalytic CO oxidation over non-noble, efficient chromia in reduced graphene oxide and graphene oxide nanocomposites, Catalysts (2020) 105.

[42] L.M. Martínez T, O. Sanz, M.I. Domínguez, M.A. Centeno, J.A. Odriozola, AISI 304 Austenitic stainless steels monoliths for catalytic applications, Chem. Eng. J. 148 (2009) 191–200.

[43] S.Y. Lee, E.W. Huang, W. Woo, C. Yoon, H. Chae, S.G. Yoon, Dynamic strain evolution around a crack tip under steady- and overloaded-fatigue conditions, Metals (Basel) 5 (2015) 2109–2118.

[44] L. Kuterasiński, P. Bodzioch, K. Dymek, R.J. Jędrzejczyk, D.K. Chlebda, J. Łojewska, M. Sitarz, G. Kurowski, P. Jeleń, P.J. Jodłowski, Spectroscopic studies of MFI and USY zeolite layers over stainless steel 316L wire gauze meshes, Spectrochim. Acta - Part A Mol. Biomol. Spectrosc. 230 (2020) 118060.

[45] F. Payri, A. Broatch, J.R. Serrano, P. Piqueras, Experimental-theoretical methodology for determination of inertial pressure drop distribution and pore structure properties in wall-flow diesel particulate filters (DPFs), Energy 36 (2011) 6731–6744.

[46] M.P. Orihuela, R. Chacartegui, A. Gómez-Martín, J. Ramírez-Rico, J.A. Becerra Villanueva, Performance trends in wall-flow diesel particulate filters: Comparative analysis of their filtration efficiency and pressure drop, J. Clean. Prod. 260 (2020) 120863.

[47] Normativa | Argentina.gob.ar, https://www.argentina.gob.ar/normativa/recurso/30389/dto779-1995-anexo1/htm (accessed February 20, 2021).

[48] C. Su, Y. Wang, A. Kumar, P.J. McGinn, Simulating real world soot-catalyst contact conditions for lab-scale catalytic soot oxidation studies, Catalysts 8 (2018) 247.

[49] M. Twigg, Controlling diesel exhaust particulate emissions, Chem. Eng. (2007) 28–31.

[50] C.J. Tighe, M. V. Twigg, A.N. Hayhurst, J.S. Dennis, The kinetics of oxidation of diesel soots and a carbon black (Printex U) by O_2 with reference to changes in both size and internal structure of the spherules during burnout, Carbon N. Y. 107 (2016) 20–35.

[51] A. Setiabudi, M. Makkee, J.A. Moulijn, The role of NO_2 and O_2 in the accelerated combustion of soot in diesel exhaust gases, Appl. Catal. B Environ. 50 (2004) 185–194.

[52] S.A. Leonardi, Tesis Doctoral - Desarrollo de papeles cerámicos catalíticos aplicados a catálisis ambiental, Universidad Nacional del Litoral, 2019.

Figure 1.

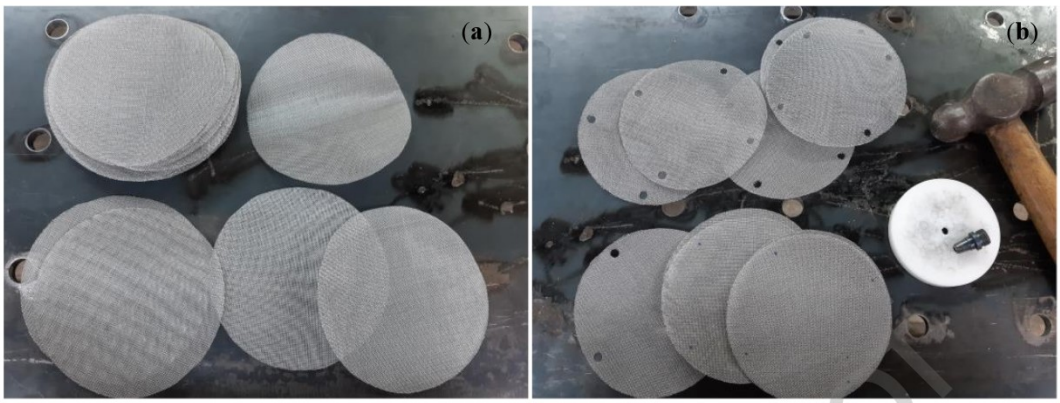

Figure 2.

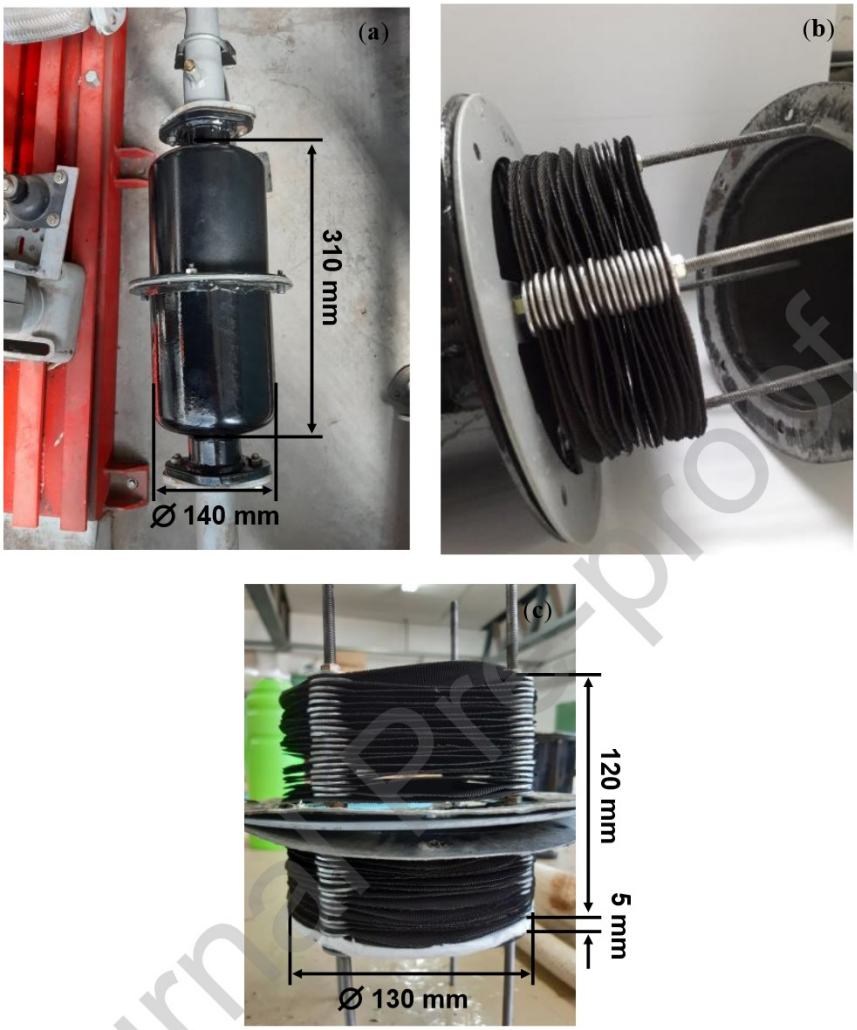

Figure 3.

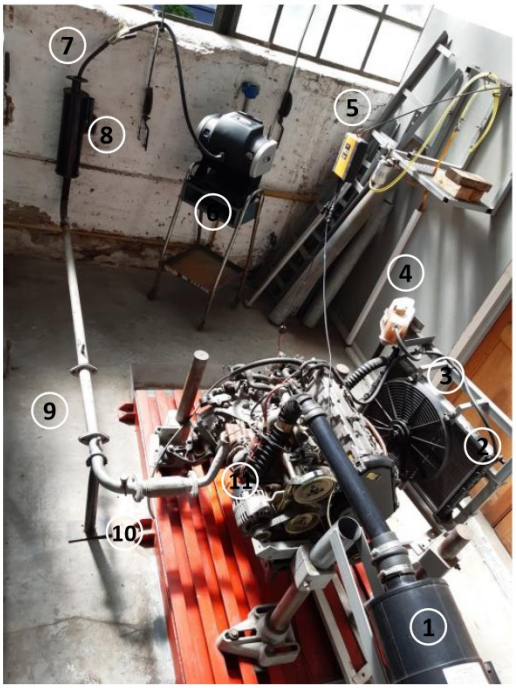

1 – Air filter
2 – Radiator
3 – Electric fan
4 – Expansion tank
5 – RC3 revolution counter
6 – Opacity meter
7 – Opacimeter sensor
8 – Muffler
9 – Section for the bench-scale monolith
10 – Bypass for the laboratory-scale samples
11 – Turbocharger

Figure 4.

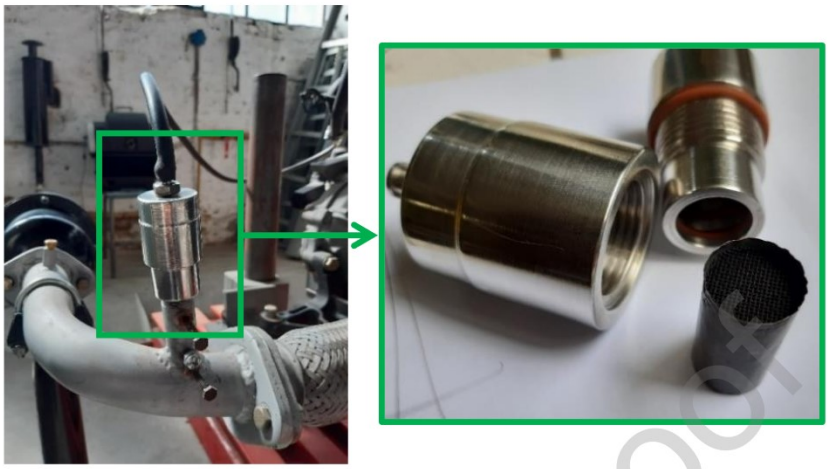

Figure 5.

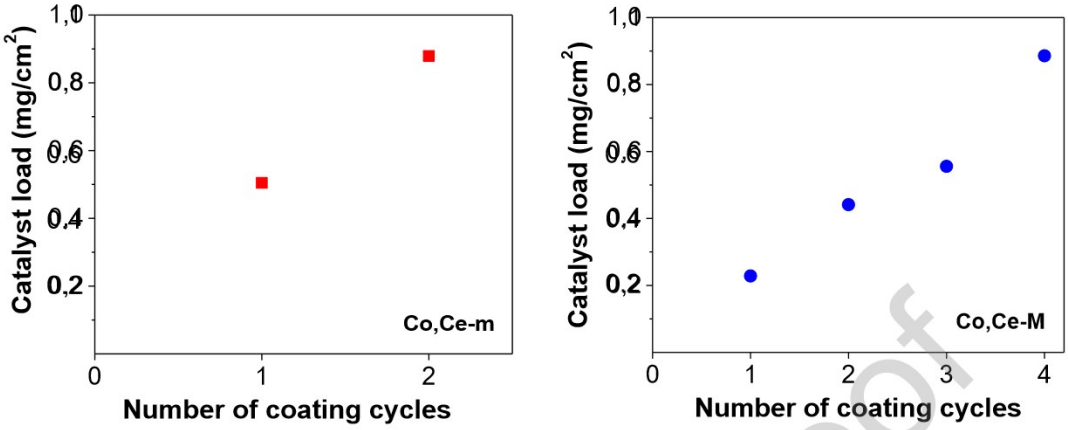

(a) **(b)**

Figure 6.

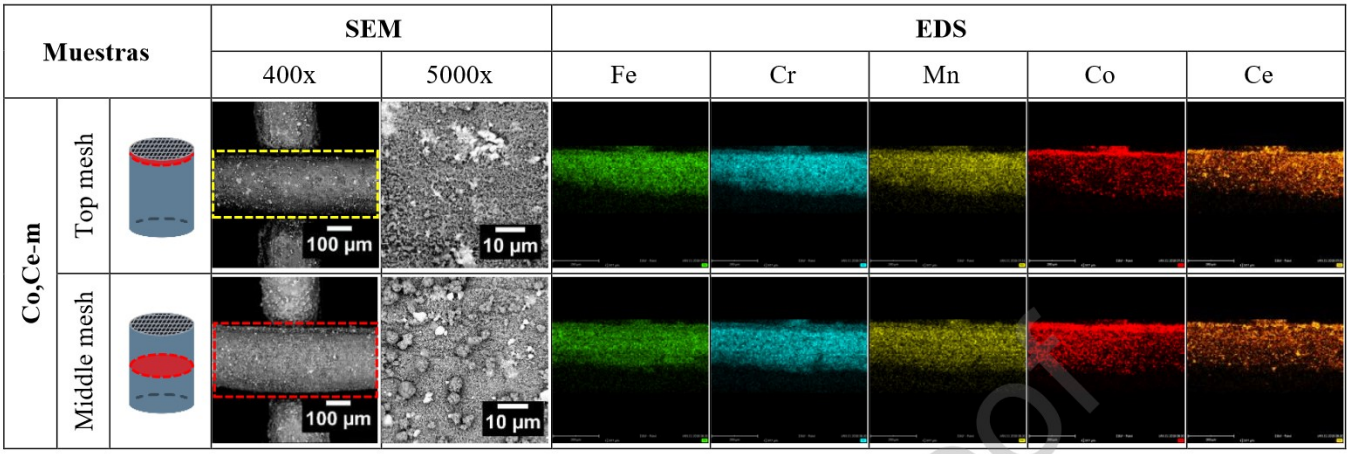

Figure 7.

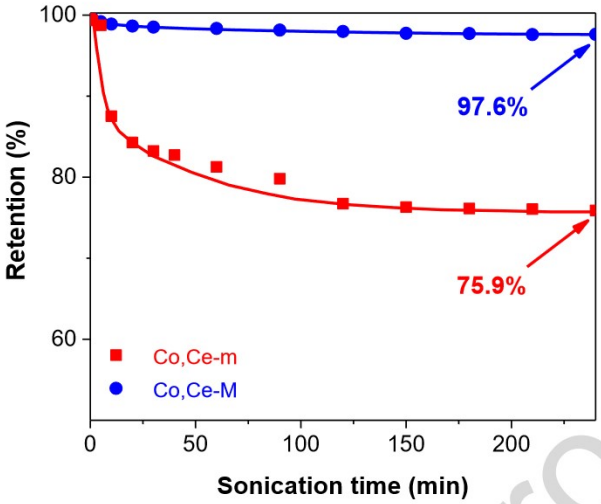

Figure 8.

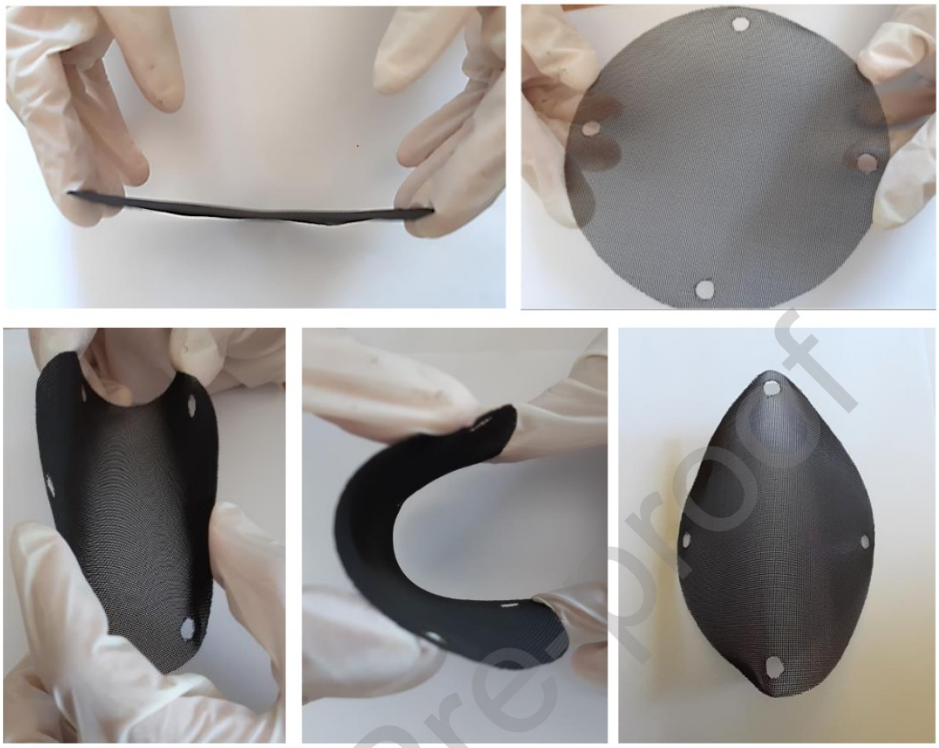

Figure 9.

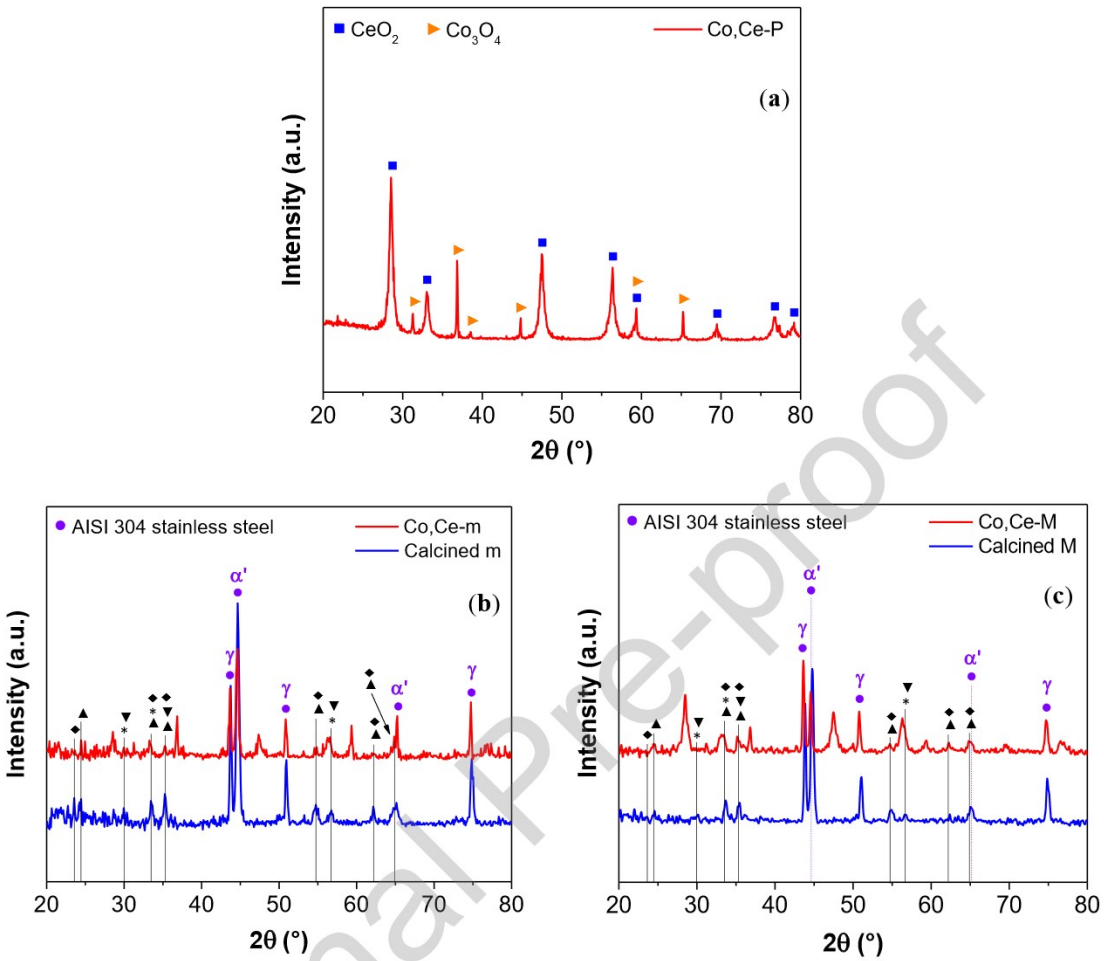

Figure 10.

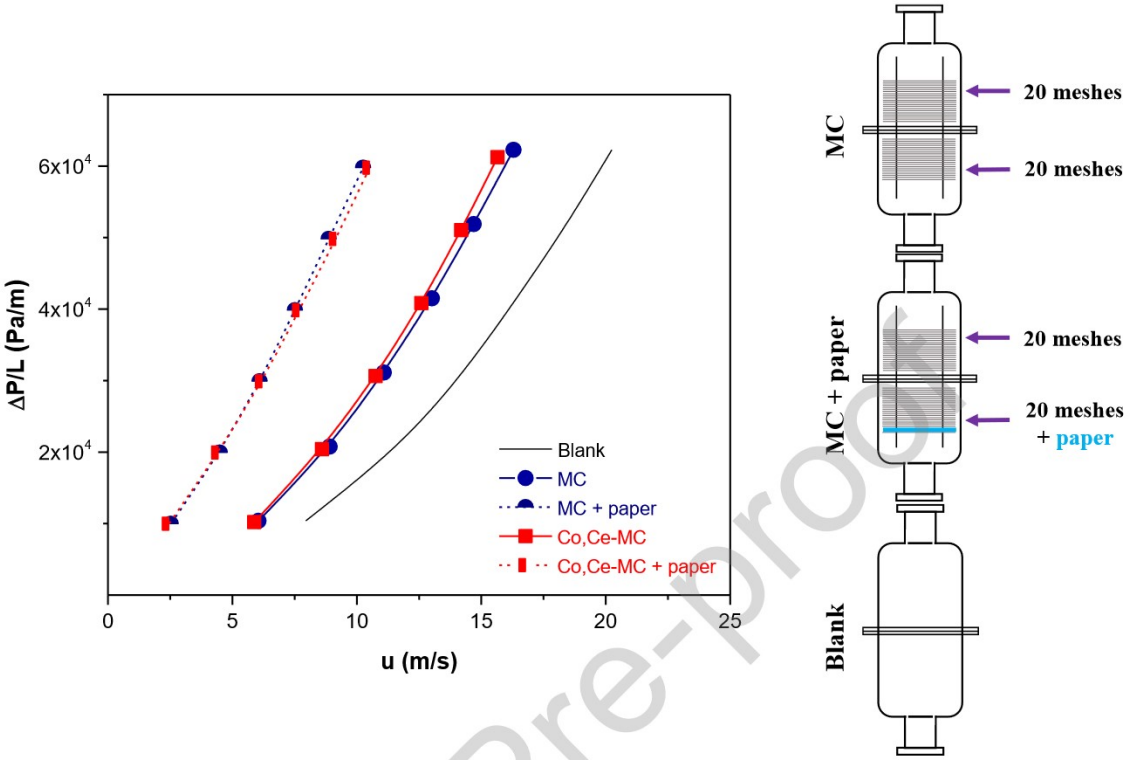

Figure 11.

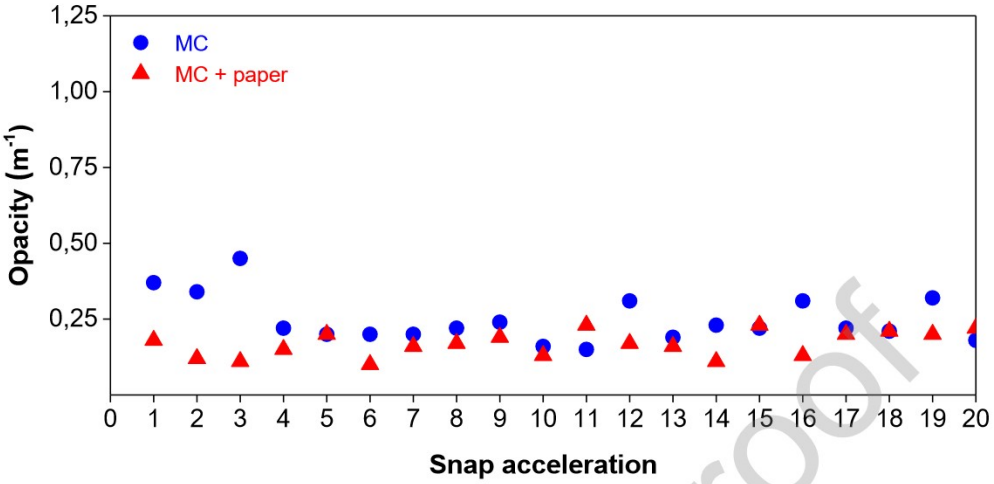

Figure 12.

Figure 13.

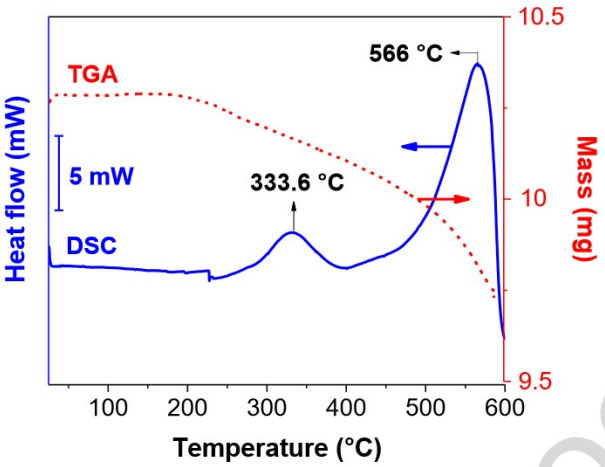

Figure 14.

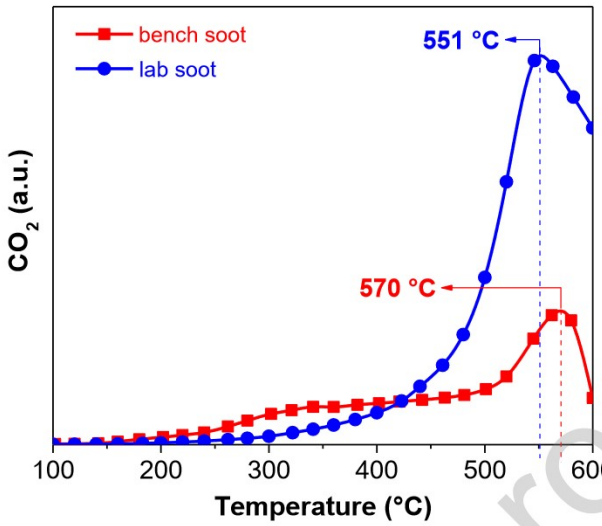

Figure 15.

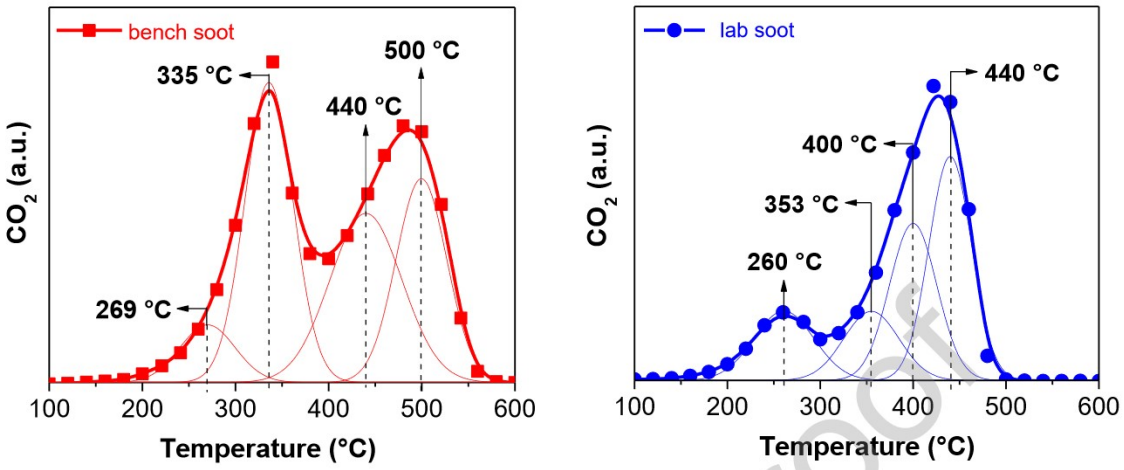

(a) (b)

Tables

Table 1.

Configuration of the scaled-up monolith	Opacity	
	N (%)	k (m^{-1})
MC	4,85	0,247
MC + paper	3,30	0,168

Figure captions

Figure 1. (**a**) Cut wire mesh discs (**b**) with four holes made with a punch.

Figure 2. Housing with stacked wire meshes inside – bench scale structure: (**a**) Structure assembled and set up on the test bench, (**b**) and (**c**) detail of the stacked meshes and ceramic paper disc that are placed in the casing.

Figure 3. Components of the diesel engine bench test.

Figure 4. Exhaust pipe bypass for laboratory-scale wire mesh monoliths.

Figure 5. Co,Ce catalyst incorporation per cm^2 of mesh into the metallic samples: (**a**) laboratory scale monolith (Co,Ce-m) and (**b**) wire meshes 130 mm diameter (average of 40 mesh discs, Co,Ce-M).

Figure 6. SEM micrographs and EDS mapping images obtained from the upper and intermediate meshes of the catalytic monolith Co,Ce-m.

Figure 7. Adherence test carried out on a wire mesh Co,Ce-monolith (Co,Ce-m – red curve) and on a 130 mm diameter Co,Ce-mesh (Co,Ce-M – blue curve).

Figure 8. Images of the Co,Ce-M wire mesh subjected to mechanical stress after the ultrasonic treatment.

Figure 9. XRD patterns obtained for (**a**) Co,Ce-P powdered catalyst, (**b**) Co,Ce-m and bare calcined monolith (Calcined m), and (**c**) Co,Ce-M and bare calcined scaled-up wire mesh (Calcined M). ●: AISI 304 stainless steel, **γ**: austenite, **α'**: martensite, ▲: Cr_2O_3, *: $Mn_{1+x}Cr_{1-x}O_{4-x}$ ▼: $FeCr_2O_4$, ◆: Fe_2O_3.

Figure 10. Pressure drop tests for different arrangements of the scaled-up monolith: without meshes (Blank); with 40 stacked mesh discs (20 meshes in each side of the housing) – with and without catalyst (Co,Ce-MC and MC, respectively) and with the adding of a ceramic paper at the end of the bed (Co,Ce-MC + paper and MC + paper).

Figure 11. Opacity values obtained at different accelerations of the diesel engine for different arrangements of the wire mesh filter: with 40 stacked meshes (MC) and with the addition of the silica-alumina paper (MC + paper)

Figure 12. Ceramic paper with particulate matter from the bench test.

Figure 13. Thermogravimetric analysis (TGA – red curve) and DSC profile (blue curve) of bench soot in air atmosphere.

Figure 14. Non-catalytic combustion of soot obtained from the test bench (bench soot) and that incorporated by means of *n*-hexane suspension (lab soot).

Figure 15. Soot combustion from the Co,Ce-m monolith with soot (**a**) from the test bench (bench soot) and (**b**) incorporated by way of a *n*-hexane suspension (lab soot).

Table 1. Measuring of the filtering capacity of the scaled-up cartridge with the test bench opacimeter. Average of measurements shown in **Fig. 11.**

CRediT authorship contribution statement

María Laura Godoy: Experimental work, analysis of data, manuscript draft. **Viviana Milt:** Project director, discussion of results, manuscript writing. **Eduardo Miró:** Analysis of data, discussion of results, manuscript writing. **Ezequiel Banús:** Analysis of data, discussion of results, manuscript writing.

Declaration of Competing **Interest**

☒ The authors declare that they have no known competing financial interests or personal relationships that could have appeared to influence the work reported in this paper.

☐The authors declare the following financial interests/personal relationships which may be considered as potential competing interests:

Highlights

- Bench scale wire mesh filter was developed by stacking 130 mm diameter mesh discs.
- Co and Ce oxide catalysts were deposited on the surface of the metallic fibers.
- The good catalytic activity would allow passive regeneration of the filter.
- Close or lower pressure drop values compared to commercial systems (SiC, ceramic).
- Robustness, versatility, low cost and excellent adhesion of the catalytic coating.